Investigation of Debris Flow Impact Mechanisms and Designs

Charles W. W. Ng, Sunil Poudyal, Haiming Liu, Aastha Bhatta, W. A. Roanga K. De Silva, and Zhenyang Jia

Abstract

Debris flows are catastrophic landslides increasing in severity in recent decades due to the more frequent and intense rainfall events under climate change. Debris flows pose a serious threat to infrastructure, settlements, and the natural environment in mountainous regions around the world causing considerable economic losses every year. To mitigate debris flows, single and multiple rigid and flexible barriers are constructed along the predicted debris flow paths. Compared with single barriers, multiple barriers are more advantageous in mitigating large debris flow volumes by progressively retaining and decelerating the flow with much smaller barrier sizes. These smaller barriers are not only easier to construct on steep hillslopes but also reduce the carbon footprint compared to large single barriers. However, current understanding of debris flow impact mechanisms on single and multiple barriers is limited due to the complex composition and scale-dependent nature of debris flow. The need of using different barrier configurations further adds to this complexity and the impact mechanisms of debris flow against single and multiple barriers are yet to be elucidated, thereby hindering the development of scientific design guidelines. This paper examines the impact mechanisms of water, dry granular and two-phase debris flows on barriers of varying stiffness, openings and numbers based on physical and numerical results, and provides recommendations for design of debris-resisting single and multiple barriers.

Keywords

Debris flow · Impact mechanisms · Rigid barrier · Basal clearance · Multiple barriers

C. W. W. Ng (✉) · S. Poudyal (✉) · H. Liu · A. Bhatta · W. A. R. K. De Silva · Z. Jia
Department of Civil and Environmental Engineering, The Hong Kong University of Science and Technology, Kowloon, Hong Kong, China
e-mail: charles.ng@ust.hk; spoudyal@connect.ust.hk

1 Introduction

Debris flows are fast-moving mixtures of rock, soil, water, and other debris, classified as flow-like landslides (Hungr et al. 2014), which can cause significant damage to infrastructure and casualties (Froude and Petley 2018). In recent years, changes in rainfall patterns due to climate change have brought more frequent and intense rainfall events with an increase in the number and severity of landslides including debris flows (Guzzetti et al. 2008; Ng et al. 2021d). Urban sprawl in hilly and mountainous areas are expected to face increased risk of landslides due to climate change (Ozturk et al. 2022; Yik et al. 2023). Between 2000 and 2019, landslides have resulted in 11% of all recorded fatalities from natural disasters with more than 70% of these fatalities occurring in Asia (Guha-Sapir 2020). Similarly, average economic losses due to landslides is US$3.5 billion every year (World Bank 2022) and is expected to increase due to climate change.

Debris-resisting barriers are commonly installed to retard and intercept debris flows from reaching further downstream. Design of these structures requires a reliable estimate of impact load as well as dimensions of openings or clearances (if any) for controlled discharge of debris flows. Current design guidelines only consider the barrier type (rigid or flexible) in their recommendations for estimating design impact force (GEO 2022; Kwan and Cheung 2012; ASI 2013; Volkwein 2014). For simplicity these guidelines prescribe empirical coefficients to consider the effects of flow composition, particle size, size of openings/basal clearances, barrier stiffness and flow-barrier interaction mechanisms on a single barrier impact force. Furthermore, the retention capacity of a single barrier may not be sufficient to arrest large debris flow volumes and require multiple barriers to be installed in a series along a drainage line to progressively impede and arrest debris flow (Huebl and Fiebiger 2005). Existing guidelines (SWCB 2019; VanDine 1996) which focus on volume retention suggest spacing between multiple

I. Alcántara-Ayala et al. (eds.), *Progress in Landslide Research and Technology, Volume 2 Issue 2, 2023*, Progress in Landslide Research and Technology, https://doi.org/10.1007/978-3-031-44296-4_17

barriers without considering flow-barrier interaction mechanisms. As a step forward, recent design recommendations (Ng et al. 2020a; Wendeler et al. 2019) and design guidelines (GEO 2022; Kwan and Cheung 2012) recommend a layer-by-layer filling of the barrier and subsequent overtopping of the barrier in design calculations by simplifying the fundamental impact mechanisms. However, the reliability of these recommendations remains poorly understood. Current understanding of flow-barrier interaction is limited because (1) debris flow impact on barriers are rarely captured in the field with enough resolution to elucidate underlying mechanisms (Takahashi 2014) (2) debris flows are scale-dependent and require unique facilities to correctly model the flow dynamics (Iverson 2015; Zhou and Ng 2010) and (3) impact dynamics of debris flows on barriers strongly depends on flow composition (Choi et al. 2015; Ng et al. 2017, 2022a; Song et al. 2017, 2018) and barrier types (Choi et al. 2016, 2020; Goodwin and Choi 2020; Ng et al. 2020b, 2022b).

In this chapter, the dynamics of debris flows and the interaction mechanisms of debris flow with different types of barriers are presented. The impact mechanisms of water, dry granular and two-phase debris flows on barriers of varying stiffness, openings and numbers are elucidated using results from physical experiments and numerical simulations. Physical experiments were conducted in multi-scale facilities including 5-m long flume and 28-m long flume. Numerical analyses revealed additional insights into the underlying impact mechanisms including evolution of granular shear strains and fluidisation of two-phase debris. Finally, improved understandings of flow-barrier interaction mechanisms from this study are consolidated into recommendations for design impact loads on single and multiple debris-resisting barriers.

2 Understanding Debris Flow-Barrier Interaction Mechanisms

2.1 Preventive Measures Against Debris Flow

Debris flow mitigation measures can be broadly classified into active and passive measures. Active measures focus on the construction of structures for flow energy dissipation, flow retention and reduction of potential risk to communities. Passive measures include risk assessment, risk monitoring and land use zoning to reduce exposure to debris flow hazards. This chapter focuses on the study of active measures, specifically, debris-resisting barriers, which can be broadly categorised as closed and open barriers. Closed barriers intercept the entire flow material preventing downstream discharge until the barrier is overtopped. Closed barriers typically include closed check dams and terminal barriers made of reinforced concrete that are constructed at the end of debris flow channels to retain the debris materials. These terminal rigid barriers are designed for large forces and for a long service life (Fig. 1).

Fig. 1 Debris resisting reinforced concrete terminal barrier (modified from Ng et al. 2020a)

In contrast, open barriers can allow controlled discharge of flow material through openings in the barrier, efficient dissipation of flow energy and partial retention of debris material. Open barriers include open check dams, rigid barriers with basal clearance (Choi et al. 2020), slit dams (Piton and Recking 2016), baffle arrays (Ng et al. 2015) and flexible barriers (Wendeler et al. 2007). Interaction mechanisms between debris flow and different types of barriers vary and need prior understanding for an effective design. The interaction mechanisms of debris flow with closed and open rigid barriers, flexible barriers and multiple barriers are elaborated next.

2.2 Debris Flow Analysis and Modelling

Figure 2 shows a strategy for analysis and modelling of debris flow impact on barriers. Modelling technique refers to tools that can be used to fulfil the specific objective of the study. Flow-barrier interaction can be modelled (1) analytically by defining simplified formulations of debris flow behaviour and its interactions with a barrier, (2) physically by using geotechnical centrifuge, laboratory or field-scale flume tests with well-defined initial and boundary conditions, and (3) numerically by using calibrated numerical models, which can provide insight into underlying physical mechanisms that cannot be observed in physical models/tests such as evolution of stresses and strains within the debris material.

To successfully derive analytical solutions for flow-barrier interaction problems, many assumptions about debris flow rheology (frictional, viscous, or two-phase mixture), debris

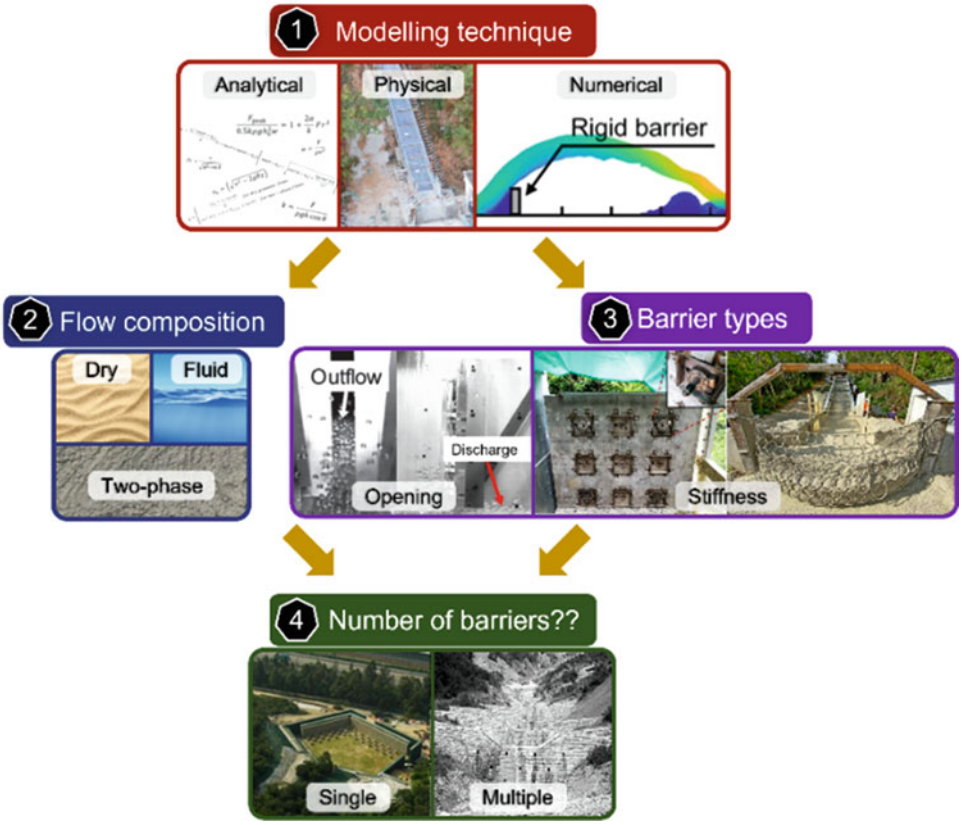

Fig. 2 A research strategy used in analysis and modelling of debris flow impact on barriers

flow regimes (uniform, steady, incompressible) and barrier stiffness (flexible or rigid) are required. While these simplifying assumptions may yield meaningful results for simple flow materials like water or dry granular flow impacting on rigid barriers, the validity of analytical solution (if any) for two-phase debris flow impact on flexible barrier is questionable (Ng et al. 2023b). Numerical modelling relaxes some of the assumptions of analytical models. While numerical modelling of different barrier rigidities may be trivial (Ng et al. 2020b), the same cannot be said about debris flow rheology. Constitutive modelling for capturing debris flow rheology is a challenging task due to the complexities involved in defining the physical interactions between solid and fluid phases (Ng et al. 2023a). Nevertheless, with the help of physical experiments, numerical models can be calibrated to reasonably capture the dynamics of debris flows despite some assumptions in the constitutive models. These calibrated numerical models can be utilised for parametric study to reveal how the stresses and strains evolve inside debris flow during impact against different kinds of barriers giving rise to different impact mechanisms. Ultimately, the results from physical experiments as well as numerical parametric studies are used to produce design guidelines for debris resisting barriers.

Depending on the barrier type (open vs closed), flow material is either completely intercepted or partially discharged through openings or allowed to overflow once the barrier is filled. If a barrier is designed to allow overflow, then instead of designing a single barrier, multiple barriers can be designed iteratively as a system. Such a multiple barrier system requires consideration of overflow and landing dynamics as well as volume retention by upstream barriers during design. These salient features of flow-barrier impact mechanisms are explored in detail in the next section.

2.3 Preventive Measures Against Debris Flow

2.3.1 Debris Flow Interaction with Single Barriers

2.3.1.1 Influence of Flow Composition

Dry granular and water flows are the two most extreme types of geophysical flows, the former governed primarily by frictional forces and the latter by viscous forces. The influence of these two extreme flow types is firstly discussed to reveal some fundamental impact mechanisms, followed by the effect of two-phase flows in impact mechanism.

Figure 3 shows a comparison of the impact kinematics of dry granular and water flows impacting against a single rigid barrier perpendicular to the ground plane (Choi et al. 2015). The tests were carried out in two different scales: (1) a 5 m-

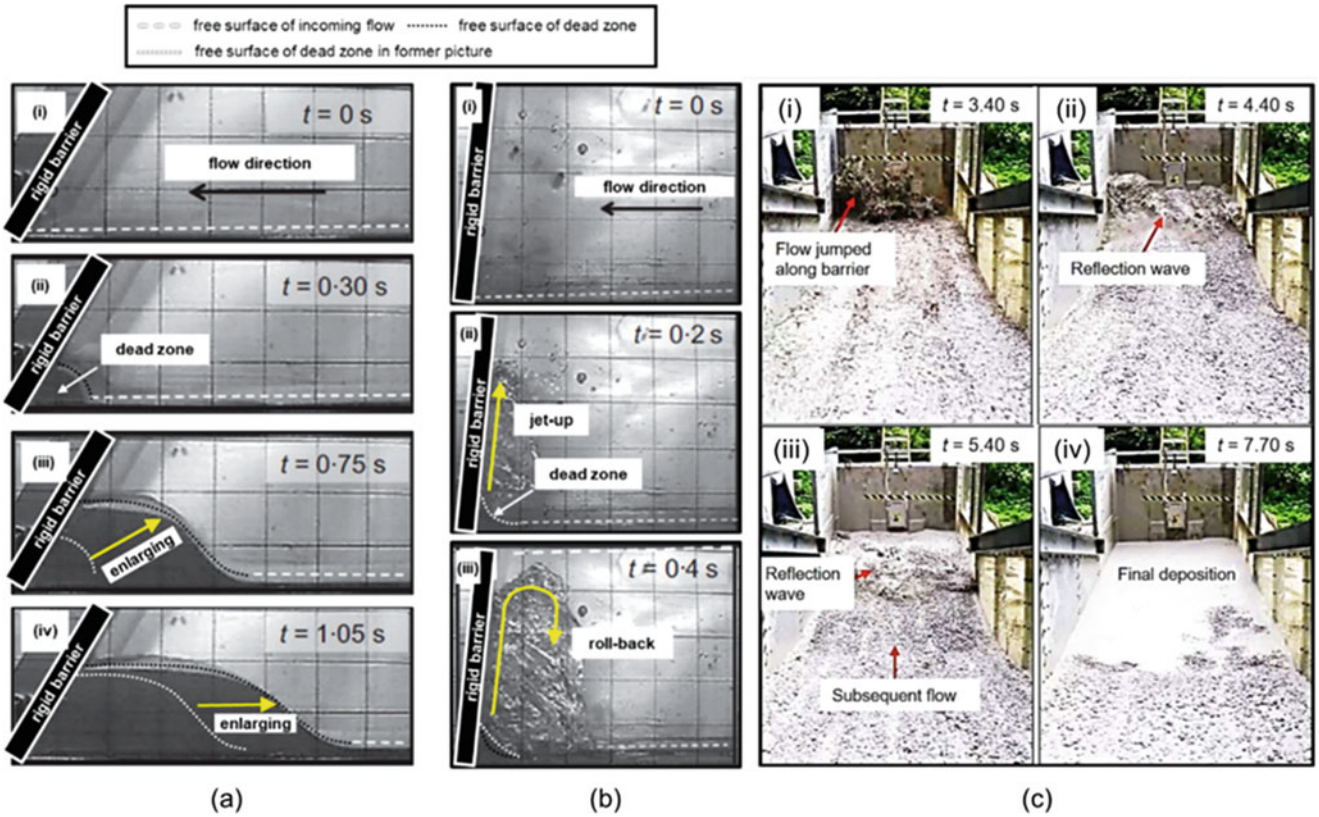

Fig. 3 Comparison of impact mechanisms for a single rigid barrier for: (**a**) dry granular flow and (**b**) water in 5 m-long flume (modified from Choi et al. 2015); (**c**) two-phase flow in 28-m long flume (Ng et al. 2021a)

long flume, inclined at 40° for dry granular (Leighton Buzzard fraction C sand; uniform grain diameters of 0.6 mm) and at 5° for water (Choi et al. 2015), and (2) a 28 m-long flume, inclined at 20° for two-phase flows (Ng et al. 2021a). In Fig. 3a (i), at $t = 0.00$ s, dry granular flow front starts to impact the barrier and gradually piles-up behind the barrier. The wedge-shaped static zone (dead zone) keeps enlarging until $t = 0.75$ s (Fig. 3a (iii)). This pile-up mechanism rapidly attenuates kinetic energy of the dry granular flow with high degree of internal and boundary friction. Furthermore, air in the interstices increases the bulk compressibility of angular sands allowing further dissipation of kinetic energy during impact. This increase in bulk compressibility can be attributed to the changes in void ratio from elastic shearing at contacts without grain crushing (Iverson 2015). As such, the dry granular flow cannot override the deposited material along the free surface and instead, the length of the dead zone keeps increasing when a granular bore propagates (piles-up) upstream at $t = 1.05$ s (Fig. 3a (iv)). For water flow (Fig. 3b), a jet-up like mechanism is observed with supercritical Fr conditions (Choi et al. 2015). Unlike the dry granular flow, the water runs up along the barrier without significant enlargement of the dead zone from $t = 0.2$ s to 0.4 s (as shown in Figs. 3b (ii) and (iii)). When kinetic energy of runup water completely transfers to gravitational potential energy, it rolls back, falls under gravity and impacts on the flume base.

Tests using dry granular and water flows are valuable in understanding fundamental impact mechanisms in purely frictional stress and viscous stress dominated regimes respectively. However, these two extreme flow types cannot model the solid-fluid interaction intrinsic to debris flows. Pore fluid regulates friction within the solid particles and at boundaries, thereby changing the amount of energy dissipation and consequently the impact mechanism (Song et al. 2017). Figure 3c shows the impact mechanism of debris flow against a single rigid barrier in the 28 m-long flume (Ng et al. 2021a). The debris material was composed of gravel, sand, clay, and water with volumetric fractions of 0.21, 0.36, 0.02, and 0.41, respectively. At $t = 3.40$ s, the flow front jumped along the barrier after impacting and is immediately reflected upstream (Fig. 3c (i)). At $t = 4.40$ s the reflected wave then propagates upstream and interacts with the incoming flow (Fig. 3c (ii)). Although the solid volume fraction of the two-phase flow is 0.59, approximately equal to that of dry granular flow in Fig. 3a, initial jet-like impact mechanism followed by reflected wave occurs rather than pile-up. Similar impact mechanisms have also been observed by Armanini et al. (2020) in 5-m long flume and Song et al. (2017) in

geotechnical centrifuge. The jet-like impact mechanism in two-phase flows can be explained by the fluidisation ratio λ (Ng et al. 2023a), which is the ratio between pore fluid pressure p_f and the total stress (sum of pore fluid pressure p_f and effective stress of solid phase p'):

$$\lambda = \frac{p_f}{p} = \frac{p_f}{p_f + p'} \quad (1)$$

Fluidisation ratio measured in 28 m-long flume tests is approximately equal to one, which implies $p' \approx 0$ and less energy is dissipated due to the low frictional force ($\mu p' \approx 0$, where μ is the friction angle of the solid phase). This can also be inferred from the horizontal free surface of the deposited debris at $t = 7.70$ s (Fig. 3c (iv)).

The distinctly different mechanisms observed for dry granular flow (pile-up) and water (vertical jet) are governed by the difference in energy dissipation in the two flow types during impact. While internal and boundary friction together with bulk compressibility rapidly reduces the flow kinetic energy for dry granular flow (Koo et al. 2017), viscous shearing in water is not as efficient in dissipating energy. These differences in impact mechanisms have a profound effect on the impact force and its distribution on a barrier (Song et al. 2017), which will be discussed in detail later.

2.3.1.2 Effects of Rigid Barrier Opening

The impact mechanisms of different flow compositions against closed rigid barriers, which are usually constructed at the exit of the debris flow channel to resist all the debris, have been discussed in previous section. On the contrary, rigid barriers are also constructed with various types of openings in the field. Piton and Recking (2016) conducted a detailed literature review on the hydraulic and deposition processes of debris flow against open rigid barriers. They summarised unique advantages of open rigid barriers compared to the closed rigid barriers as follows: (1) regulating peak flow rate; (2) increasing energy dissipation; (3) filtering and storing unwanted components, such as separating bed-load sizes or grading wood. Aside from the functioning perspectives of open rigid barriers, the design of these barriers also requires the knowledge of impact force. As such, the discharge of open rigid barriers is discussed in this section and the recommendation of design impact force for open rigid barriers is provided in Sect. 3.

The efficiency of open rigid barriers in dissipating the flow energy can be controlled by designing a basal clearance, which is an opening between the base of the barrier and channel bed, such that the impact force on downstream barriers can be optimised (Choi et al. 2020; Ng et al. 2022b; Liu et al. 2023). By designing a basal clearance, the peak flow discharge rate can be regulated.

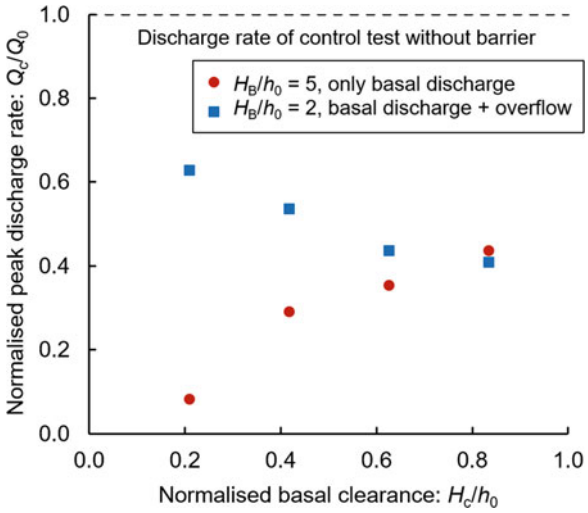

Fig. 4 Influence of basal clearance height on the peak discharge rate

Figure 4 shows the physical test results of peak basal discharge rate Q_c of dry granular flow composed of 3-mm glass beads impacting on rigid barrier with a normalised basal clearance H_c/h_0 ranging from 0.2 to 0.8 (Ng et al. 2022b). In the tests, two barrier heights perpendicular to the channel slope were adopted with five times the flow depth ($H_B/h_0 = 5$) and twice the flow depth ($H_B/h_0 = 2$). The peak discharge rate through the basal clearance is normalised by the peak discharge rate of a control test without barrier. For the tests with $H_B/h_0 = 5$, the large barrier height prevents overflow, and thus the discharge rate is dominated by basal discharge and increases with the increase in basal clearance height. In contrast, when barrier height is lower at $H_B/h_0 = 2$, both overflow and basal discharge occur and influence the downstream discharge rate. With the increase of basal clearance, the peak discharge rate decreases due to the reduced overflow and when H_c/h_0 reaches 0.8, the peak discharge is dominated by basal discharge rather than the overflow. Liu et al. (2023) proposed a new dimensionless number named as overflow number to characterise whether the downstream discharge is dominated by basal discharge or overflow. The overflow number N_{of} is expressed as follows:

$$N_{of} = \frac{h_j}{H_B}\left(1 - \frac{H_c}{h_0}\right) \quad (2)$$

where h_j is the runup height calculated by the momentum-based model (Liu et al. 2023). By comparing the physical and numerical results, the study found that the basal discharge dominates the peak discharge when $N_{of} < 1$, while the overflow dominates when $N_{of} > 1$. A threshold value of $N_{of} = 1$ can be used to optimise the design of the barrier by maximising dissipation of the flow energy.

In addition to discharge, the impact force induced on open barrier by debris flow requires attention and will be discussed later.

2.3.1.3 Role of Barrier Stiffness

After considering the effects of debris flow composition and barrier opening on impact mechanisms, this section discusses the effects of barrier deformation during impact. Ng et al. (2020b) studied the impact of dry granular flows against a deformable cantilever barrier using material point method (MPM). The MPM model was calibrated using flume test results reported in Ng et al. (2017). The calibrated model was then utilised in carrying out a numerical parametric study to investigate how the stiffness of the barrier affects barrier impact force, barrier deformation and energy dissipation during impact. The investigated stiffness (flexural rigidity) ranged from a stiff 1 m-thick concrete barrier ($EI = 4.17 \times 10^8$ N · m^2) to highly flexible 2 mm-thick steel barrier ($EI = 8.33$ N · m^2). To facilitate direct comparison with a 1 m-thick reinforced concrete barrier, the flexural rigidities of all the investigated barriers were normalised by the flexural rigidity of 1 m-thick and 3 m-tall reinforced concrete barrier. The normalised flexural rigidity ratio ($3EI/H^3_{\text{norm}}$) of the 1-m thick and 3 m-tall reinforced concrete barrier is 1.0 while that of the 2 mm-thick steel barrier is 2.5×10^{-6}.

Figure 5 shows the influence of barrier flexural rigidity ratio on the impact force and final barrier deformation. The abscissa shows the normalised flexural rigidity ratio. The ordinate on the left shows peak barrier deformation $D_{\max}$ along the impact direction normalised by the barrier height H. The ordinate on the right shows the impact force normalised by computed impact force on a 1 m-thick reinforced concrete barrier. The computed results reveal that the normalised impact force reduces nonlinearly as the flexural stiffness reduces. Particularly, a 2 mm-thick steel barrier ($3EI/H^3_{\text{norm}} = 2.5 \times 10^{-6}$) can reduce impact force by 60% while deforming around 40% of the barrier height in the direction of impact compared to a 1 m-thick reinforced concrete barrier that is essentially rigid. This implies, lowering the stiffness of a barrier effectively reduces peak impact force.

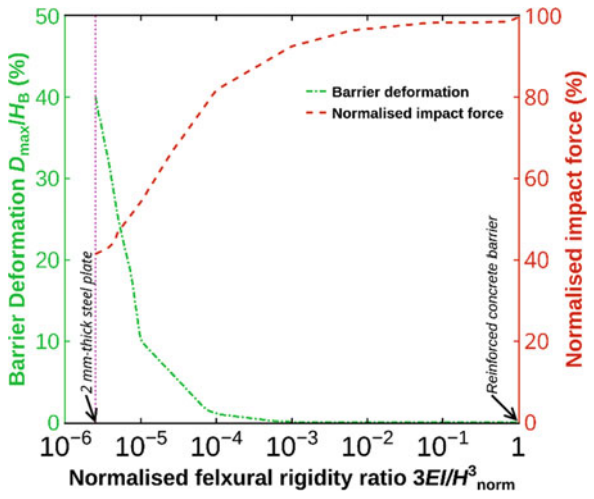

Fig. 5 Normalised barrier impact force and peak barrier deformation against normalised barrier flexural rigidity for dry sand flow impact on deformable barriers (redrawn from Ng et al. 2021c)

Figure 6a, b show how and why the granular flow impact force decreases as the barrier flexural rigidity reduces. These figures compare the accumulated equivalent shear strain of dry sand mass after impacting steel barriers of 2 mm and 5 mm thickness, respectively. The 2 mm-thick steel barrier undergoes (Fig. 6a) more significant deformation upon impact, leading to more distinct shear bands in the sand deposit compared to the 5 mm-thick steel barrier (Fig. 6b). In the 5 mm-thick barrier, the accumulated equivalent shear strain is only noticeable along the boundaries. This suggests that the flow experiences less shearing deformation after impact because of the smaller deflection of the stiffer 5 mm-thick steel barrier.

This section presented the influence of barrier stiffness on reduction of impact force from dry sand flow. A unified approach for estimating the design impact force on rigid and flexible barriers will be discussed later.

2.3.2 Debris Flow Impact on Multiple Barriers

The previous discussions only focused on how debris flows affect a single barrier to reveal the underlying impact mechanisms. To mitigate large volumes of debris flow by retaining debris along its path, however, multiple barriers need to be installed in the flow channel. In addition to impact, multiple barriers require investigation of overflow and landing mechanisms. Downstream barriers should also consider the effects of upstream barriers on debris flow dynamics and

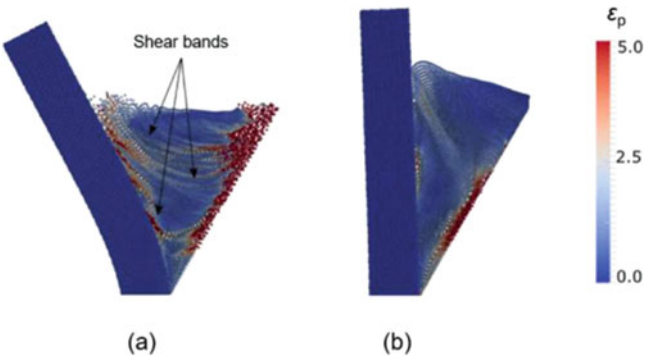

Fig. 6 Equivalent shear strain (ε_p) contour and shear bands within dry sands behind (**a**) 2 mm-thick steel barrier ($3EI/H^3_{\text{norm}} = 2.5 \times 10^{-6}$) (**b**) 5 mm-thick steel barrier ($3EI/H^3_{\text{norm}} = 1.0 \times 10^{-4}$) (redrawn from Ng et al. (2020b))

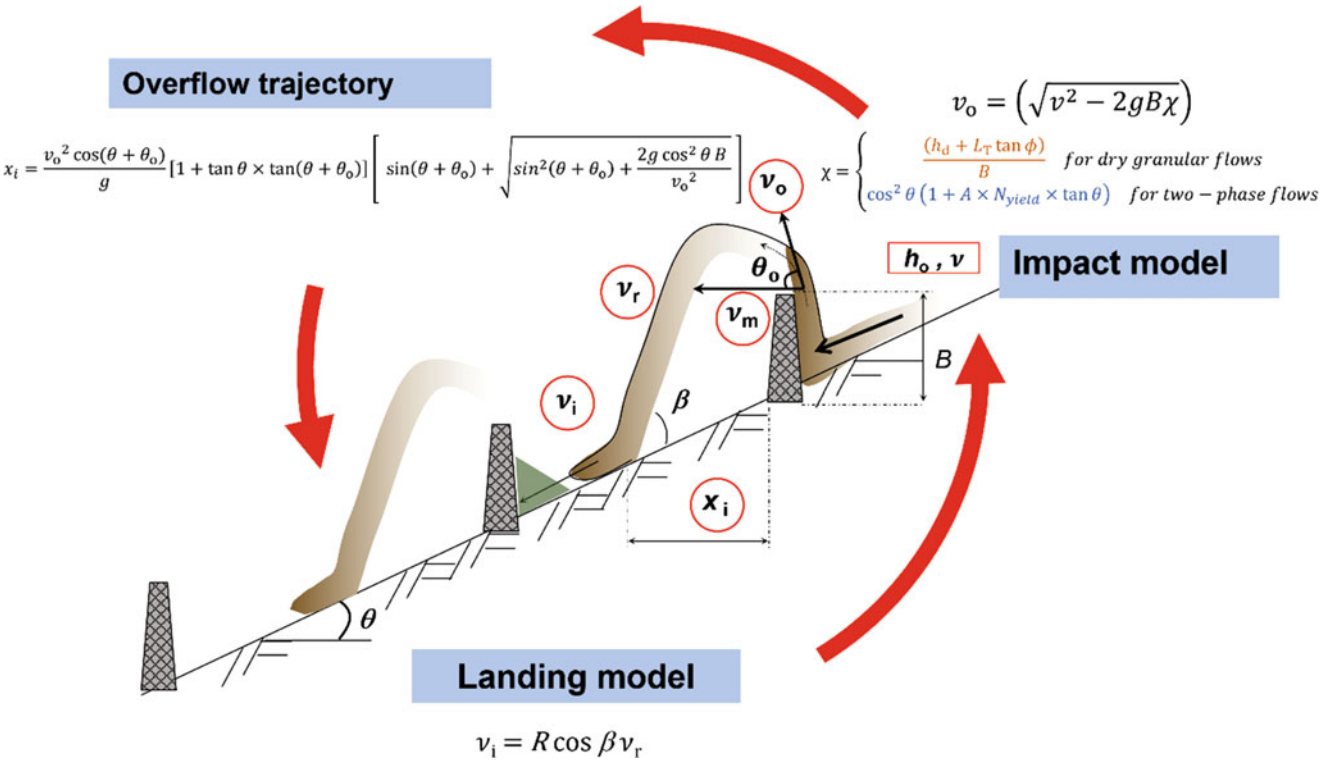

Fig. 7 A schematic diagram of the multiple barrier framework for both dry granular and two-phase flows. The framework includes (1) impact model, (2) overflow and landing kinematics, and (3) subsequent barrier impact

volume retention. Early designs of multiple barriers mainly focused on the volume of debris retained by each barrier, slowing down the flow and stabilising the channel gradient (VanDine 1996). However, this approach neglects the interaction between the flow and barriers (Kwan et al. 2015). An analytical model for a multiple barrier framework has been developed to rationally define barrier spacing, considering velocity attenuation during flow-barrier interaction, defining overflow trajectory, and calculating the velocity after landing that impacts the downstream barrier (Ng et al. 2019). Recently, it was found that contrary to the accretion of flowing grains along the free surface of the deposited material in dry granular flow, debris flow dissipates energy during flow-barrier interaction through internal shearing (Ng et al. 2022a). Debris flow is also found to launch at an angle that results in higher overflow distance requiring larger barrier spacing to prevent overflow from directly impacting or overtopping the subsequent barrier. Furthermore, it was also recently found that the equivalent fluid model may not accurately represent the reduction in friction coefficient between the flow and the bed after landing as it ignores the excess pore pressure generated in fluid phase (Ng et al. 2023a). In light of the new findings the existing multiple barrier framework from Ng et al. (2020a) has been updated to capture salient features of impact and overflow mechanisms for different flow types as shown in a schematic diagram in Fig. 7.

The updated multiple barrier framework in Fig. 7 shows a process-based approach to the design of multiple debris resisting barriers. Analytical equations are used to capture the three key processes of debris flow impact, overflow and landing based on impact mechanisms for different flow types. The framework can be used iteratively to design a series of barriers in the channel to resist a predefined volume of debris flow. Details of the updated multiple barrier framework, primarily the new changes to the existing framework of Ng et al. (2020a) are shown below.

2.3.2.1 Initial Impact Mechanism: Quantifying Energy Dissipation During Pile-Up and Run-Up

The first design step for multiple barriers is to determine energy dissipation at the first barrier and hence define overflow velocity (v_o). As explained earlier, flow can either pile-up, form jump or run-up depending upon the flow composition (Fig. 3). The energy dissipation also differs depending on the mechanism of flow-barrier interaction. For dry granular flows, pile-up mechanism occurs, and energy dissipates due to friction between the deposited and incoming flows. Velocity attenuation model proposed by Koo et al. (2017) can provide energy dissipation in dry granular flows and obtain overflow velocity. Since two-phase flows exhibit a jump or run-up mechanism during flow-barrier interaction, layer by layer frictional dissipation cannot be used. Ng et al. (2022a)

suggests an approach to define energy dissipation for two-phase flows based on yield stress of the interstitial fluid. These two approaches of estimating flow kinetic energy dissipation during barrier interaction can be unified while calculating overflow velocity as follows:

$$v_o = \sqrt{v^2 - 2gB\chi} \tag{3}$$

where,

$$\chi = \begin{cases} \dfrac{(h_d + L_T \tan\phi)}{B} \\ \textit{for dry granular flows} \\ \cos^2\theta\left(1 + A \times N_{yield} \times \tan\theta\right) \\ \textit{for two-phase flows} \end{cases} \tag{4}$$

where, v_o is the overflow velocity at the crest of the barrier, g is the acceleration due to gravity, $B = H_B/\cos\theta$ is the vertical height of the barrier, H_B is the height of the barrier perpendicular to the channel inclination, θ is the slope inclination and χ is the flow kinetic energy dissipation, which depends on flow composition. For dry granular flows, h_d is the height of the deposited granular material, L_T is the length of the free surface of arrested granular material and ϕ is the friction angle. For two-phase flows, A is an empirical coefficient that considers the extent of internal shearing in the flow material in proportion to the yield stress of the interstitial fluid (τ_y). $N_{yield} = \tau_y/\rho g h \sin\theta$ is the dimensionless yield stress of the flow, which is the ratio of yield stress of the interstitial fluid and the driving shear stress component parallel to the slope. $A \times N_{yield}$ gives the dissipation of kinetic energy within the two-phase flow.

2.3.2.2 Overflow Trajectory and Landing Distance

Ng et al. (2019) assumes that overflow occurs horizontally from the crest of the barrier. This is true for the flow with pile-up mechanism. This assumption provides conservative estimate for the case when the flow overflows at an angle below the horizontal level. However, when the flow launches at an angle (θ_o) with horizontal, overflow distance increases compared to the horizontal launch (Ng et al. 2022a). An overflow trajectory as shown in Fig. 7 can be used to define the landing distance (x_i). Equation (5) provides formulation to calculate the minimum barrier spacing based on this overflow distance.

$$x_i = \frac{{v_o}^2 cos(\theta + \theta_o)}{g}[1 + \tan\theta \times \tan(\theta + \theta_o)] \times \left[\sin(\theta + \theta_o) + \sqrt{\sin^2(\theta + \theta_o) + \frac{2g\cos^2\theta B}{{v_o}^2}}\right] \tag{5}$$

For dry granular flows or for the cases where overflow occurs horizontally, the above equation transforms into the overflow equation given by Kwan et al. (2015) as:

$$x_i = \frac{{v_m}^2}{g}\left[\tan\theta + \sqrt{\tan^2\theta + \frac{2gB}{{v_m}^2}}\right] \tag{6}$$

Once the overflow lands on the bed, velocity of landed flow can be calculated by using Eq. (7):

$$v_i = R\cos\beta v_r \tag{7}$$

where v_r is calculated by using the overflow trajectory as used in obtaining Eq. (5). This velocity is then used as impact velocity for the downstream barrier.

After landing, landed flow is assumed to flow with a velocity (v_i) and flow depth (h_o) and impact the subsequent barrier. The impact model (Eq. 3) is again applied to obtain overflow velocity and the process continues until the debris flow comes to a stop. Ng et al. (2023a) numerically investigated behaviour of two-phase flow of 500 m^3 volume impacting two barriers. The computed results reveal that equivalent fluid models such as 3d-DMM (Koo et al. 2018) and DAN3D (McDougall and Hungr 2004), commonly used for debris flow analysis can underpredict the impact velocity and impact force at the second barrier. This is because when the overflow lands, it induces rapid undrained loading during impact increasing the pore fluid pressure within the landed flow (Ng et al. 2023a). This excess pore fluid pressure cannot be captured by equivalent fluid model. The increase in pore fluid pressure reduces effective basal friction (Eq. 1) resulting in flow acceleration, increased impact velocity at the barrier and hence increased impact force on the downstream barriers.

3 Design Recommendations for Debris Resisting Barriers

3.1 Debris Flow Impact Force on Barriers

Current state of understanding of impact mechanisms of debris flows can be reflected in international design guidelines (ASI 2013; CAGHP 2018; GEO 2022; NILIM 2016; SWCB 2019; Volkwein 2014). These international guidelines assume debris flows behave as continuum fluids. Debris flow impact forces on barriers are estimated using equilibrium of forces in hydrostatic models and conservation of linear momentum in hydrodynamic models. Although these international design guidelines predominantly considered hydrodynamic model only while estimating barrier impact force, multiple researchers have shown that both the

Table 1 Summary of dynamic impact coefficient (α) in international design guidelines

Region	Dynamic impact coefficient (α) (for soil debris impact on rigid barrier)	References
Canada	1.00	Hungr et al. (1984)
Mainland China	1.33 (for rectangular barrier) 1.47 (for square barrier)	CAGHP (2018)
Taipei, China	1.00	SWCB (2019)
HKSAR, China	1.50	GEO (2022)
Japan	1.00	NILIM (2016)
Austria	1.00	ASI (2013)

hydrostatic and hydrodynamic forces should be considered for wide range of impact scenarios (Armanini and Scotton 1992; Ng et al. 2020a; Song et al. 2017). Including both the hydrostatic and hydrodynamic forces, the total impact force exerted by debris flow can be expressed as:

$$F_{\text{peak}} = F_{\text{dynamic}} + F_{\text{static}} = \alpha\rho v^2 hw + 0.5k\rho g h^2 w \quad (8)$$

where α and k are the dynamic and static impact coefficients, respectively; is the flow density; v is the velocity of the flow; h is the flow depth and w is the channel width. While all the design guidelines assume $k = 1.0$ by neglecting the shear strength of fluidised debris, there is no consensus on the value of dynamic impact coefficient α as shown in Table 1.

Rearranging Eq. (8) gives normalised impact force on the barrier with respect to the hydrostatic force of debris flow as follows:

$$\frac{F_{peak}}{0.5k\rho g h^2 w} = 1 + \frac{\alpha v^2}{0.5kgh} \quad (9)$$

Simplifying the Eq. (9) by expressing the Froude number as $Fr = v/\sqrt{gh}$,

$$\frac{F_{peak}}{F_{static}} = 1 + \frac{2\alpha}{k} Fr^2 \quad (10)$$

Equation (10) can be used as a unified approach for estimating the design impact force on debris resisting barriers. In Eq. (10), if α is assumed to be unity, then the impact scenario is inelastic. However, if α is assumed to be two, then the impact scenario is elastic (Ng et al. 2019). Assuming an isotropic stress distribution within the debris material, the hydrostatic impact coefficient becomes $k = 1$ (Ng et al. 2021b). An increase of normalised impact force means the dynamic impact force has a higher contribution towards the peak impact force compared to hydrostatic force.

Figure 8 shows normalised impact force exerted by debris flows for different Froude conditions. In Fig. 8a, the analytical equations with $k = 1.0$; $\alpha = 1.5$ correspond to the design recommendation by Ng et al. (2020a), which was also recently adopted in Hong Kong for debris resisting rigid barriers (GEO 2022). It is worthwhile to note that $k = 1.0$; $\alpha = 1.5$ provides a theoretical upper-bound for impact force on single rigid barrier for all types of investigated flows: water, two-phase (Liu 2019) and dry granular (Zanuttigh and Lamberti 2006). Another theoretical bounding line using Eq. (10) with $k = 1.0$; $\alpha = 1.0$ provides an upper bound for all data points of flexible barriers impacted by two-phase flow. Given that the existing design guideline in Hong Kong for debris resisting flexible barriers stipulates $k = 1.0$; $\alpha = 2.0$, there are prospects of load optimisation for flexible barrier design. Similarly, normalised peak impact force from dry granular flows on rigid barrier with basal clearance is also shown. The basal clearance H_c is normalised by the maximum flow depth h_0 and reported in the figure alongside the data points. The theoretical bounding line with $k = 1.0$; $\alpha = 1.0$ also provides a conservative estimate of impact force for basal clearances ($H_c/h_0 \leq 1.0$) and can be adopted for designing rigid barriers with a basal clearance.

Figure 8b shows the changes in the normalised peak impact force with flow Froude number (Fr) for the second rigid barrier of a dual barrier system. Measured as well as computed results are used in evaluating the design impact criteria for second barrier in a dual barrier system. Similar to Fig. 8a, the measured peak impact forces (F_{peak}) for dry granular flows and water are normalised by the theoretical static force (F_{static}) $0.5k\rho g h_0^2 w$. The flow depth before impacting the second barrier is assumed to remain constant and equal to the flow depth at the first barrier for a conservative estimate of impact forces on the second barrier. Measured data from 5 m-long flume experiments using water and dry granular flow and computed results from design case in Hong Kong using two-phase flow are compared. Dry granular flows have lower Froude numbers than water flows because there is more energy dissipation via frictional shearing among the grains (Choi et al. 2015).

Water flows exert higher normalised impact forces compared to dry granular flows because the water overflow lands closer to the first barrier, allowing for sufficient length for flow acceleration (Ng et al. 2020a). The measured impact forces are compared with a theoretical equation for peak impact force (Eq. 10). In comparison with the upper bound for a single rigid barrier (Fig. 8a), $k = 1.0$; $\alpha = 1.5$, an upper bound with $k = 1.0$; $\alpha = 1.0$ provides a conservative estimate

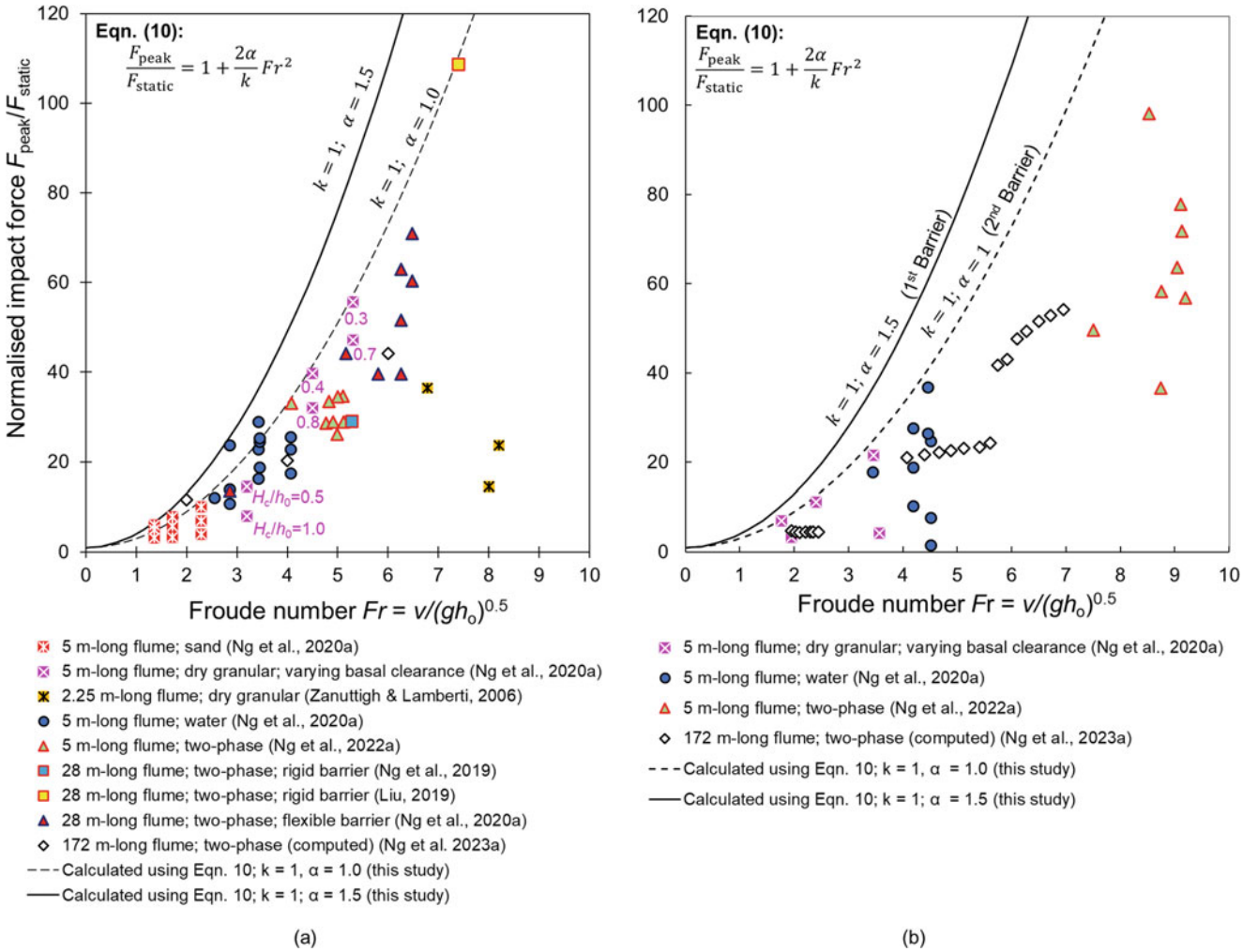

Fig. 8 Design impact force at different Froude numbers for (**a**) single barrier (rigid closed, rigid with basal clearance and flexible) (**b**) first and second rigid barrier in dual barrier system (modified from Ng et al. 2020a)

of the impact force exerted on the second barrier. The reduction in normalised peak impact forces for the second barrier is mainly due to energy dissipation during impact on the first barrier and landing between the dual barriers. Design recommendations by Ng et al. (2020a) have been verified with additional experimental and numerical results and are summarised in Table 2.

4 Summary and Conclusions

Current state-of-the-art research on the impact mechanisms of debris flows has been reviewed and discussed in this chapter. This study emphasises how debris flow composition, barrier opening, barrier stiffness and number of barriers govern the debris flow impact dynamics. The following key findings are summarised from this study:

1. Debris flow composition governs the mechanism of impact on barriers. Dry granular flows exhibit a pile-up mechanism with progressive deposition of material behind the barrier during impact. The flow kinetic energy is dissipated via sustained shearing between grains and large bulk compressibility when the grains are angular. In contrast, water and fluidised two-phase flows show a jet-like runup mechanism. While energy is dissipated solely through viscous shearing in water flows, concentration of solids in two-phase flow dictates whether energy is dissipated by frictional, collisional, and viscous stresses within the flow.
2. Newly proposed dimensionless overflow number N_{of} with a threshold value of 1.0 should be used to design rigid barrier with basal clearance ($0.2 \leq H_c/h_0 \leq 0.8$) to regulate discharge of debris material downstream while reducing the impact force.
3. Impact force exerted on a barrier reduces nonlinearly with the stiffness of the barrier. Compared to a 1-m thick reinforced concrete barrier, a deformable barrier of 2 mm thick steel plate cantilevered at the base experiences only 40% of the impact force.

Table 2 Design recommendations for estimating the impact loads for different barrier configurations (modified from Ng et al. 2020a)

Design recommendations[a]	Dynamic impact coefficient (α)
Single rigid barrier without basal clearance	1.5
Single rigid barrier with basal clearance ($0.3 \leq H_c/h_0 \leq 1.0$)	1.0
Single flexible barrier	1.0
Second rigid barrier in a dual rigid barrier system	1.0

[a] A static impact coefficient $k = 1.0$ is recommended to deduce static load

4. Design loads for a single closed rigid barrier should be estimated using $\alpha = 1.5$ with static load estimated using $k = 1.0$. For a single rigid barrier with basal clearance ($0.3 \leq H_c/h_0 \leq 1.0$), single flexible barrier, and the second barrier in a dual rigid barrier system design load should be estimated using $\alpha = 1.0$ with static load estimated using $k = 1.0$. It is worth noting that these design recommendations are for continuum-like debris material and do not consider discrete impacts from a single boulder or a cluster of boulders. As such, other design guidelines can provide higher α values compared to this study.

Acknowledgments The authors are grateful for financial support from the area of excellence project grant AoE/E-603/18 provided by the Research Grants Council (RGC) of the Government of Hong Kong Special Administrative Region (HKSAR), China. S. Poudyal, A. Bhatta and W.A.R.K. De Silva gratefully acknowledge the support from Hong Kong PhD Fellowship Scheme award provided by RGC of HKSAR.

References

Armanini A, Scotton P (1992) Experimental analysis on the dynamic impact of a debris flow on structures. In: Proceedings of International Symposium on Interpreavent, pp 107–116

Armanini A, Rossi G, Larcher M (2020) Dynamic impact of a water and sediments surge against a rigid wall. J Hydraul Res 58(2):314–325. https://doi.org/10.1080/00221686.2019.1579113

ASI (2013) ONR 24801 protection works for torrent control – static and dynamic actions on structures. Vienna, Austrian Standards Institute, p 32

CAGHP (2018) Specification of design for debris flow prevention (T/CAGHP 021–2018). China University of Geosciences Press, Wuhan

Choi CE, Au-Yeung SCH, Ng CWW, Song D (2015) Flume investigation of landslide granular debris and water runup mechanisms. Géotechnique Lett 5(1):28–32. https://doi.org/10.1680/geolett.14.00080

Choi CE, Goodwin SR, Ng CWW, Cheung DKH, Kwan JSH, Pun WK (2016) Coarse granular flow interaction with slit structures. Géotechnique Lett 6(4):267–274. https://doi.org/10.1680/jgele.16.00103

Choi CE, Ng CWW, Liu H, Wang Y (2020) Interaction between dry granular flow and rigid barrier with basal clearance: analytical and physical modelling. Can Geotech J 57(2):236–245. https://doi.org/10.1139/cgj-2018-0622

Froude MJ, Petley DN (2018) Global fatal landslide occurrence from 2004 to 2016. Nat Hazards Earth Syst Sci 18(8):2161–2181. https://doi.org/10.5194/nhess-18-2161-2018

GEO (2022) GEO Technical Guidance Note No. 52 (TGN 52) Enhanced Technical Guidance on Design of Rigid Debris-resisting Barriers. Geotechnical Engineering Office, Civil Engineering and Development Department, The Government of the Hong Kong Special Administrative Region, Hong Kong SAR, 10 p

Goodwin GR, Choi CE (2020) Slit structures: fundamental mechanisms of mechanical trapping of granular flows. Comput Geotech 119:103376. https://doi.org/10.1016/j.compgeo.2019.103376

Guha-Sapir D (2020) CRED (2020) EM-DAT: the emergency events database. Université catholique de Louvain (UCL), Université catholique de Louvain (UCL)

Guzzetti F, Peruccacci S, Rossi M, Stark CP (2008) The rainfall intensity–duration control of shallow landslides and debris flows: an update. Landslides 5(1):3–17. https://doi.org/10.1007/s10346-007-0112-1

Huebl J, Fiebiger G (2005) Debris-flow mitigation measures. In: Jakob M, Hungr O (eds) Debris-flow hazards and related phenomena. Praxis Springer, Berlin, pp 445–487

Hungr O, Morgan GC, Kellerhals R (1984) Quantitative analysis of debris torrent hazards for design of remedial measures. Can Geotech J 21(4):663–677. https://doi.org/10.1139/t84-073

Hungr O, Leroueil S, Picarelli L (2014) The Varnes classification of landslide types, an update. Landslides 11(2):167–194. https://doi.org/10.1007/s10346-013-0436-y

Iverson RM (2015) Scaling and design of landslide and debris-flow experiments. Geomorphology 244:9–20

Koo RCH, Kwan JSH, Ng CWW, Lam C, Choi CE, Song D, Pun WK (2017) Velocity attenuation of debris flows and a new momentum-based load model for rigid barriers. Landslides 14(2):617–629. https://doi.org/10.1007/s10346-016-0715-5

Koo RCH, Kwan JSH, Lam C, Goodwin SR, Choi CE, Ng CWW, Yiu J, Ho KKS, Pun WK (2018) Back-analysis of geophysical flows using three-dimensional runout model. Can Geotech J 55(8):1081–1094. https://doi.org/10.1139/cgj-2016-0578

Kwan JSH, Cheung RWM (2012) Suggestions on design approaches for flexible debris-resisting barriers, Discussion note no. DN 1/2012. Geotechnical Engineering Office HKSAR, Hong Kong, 91 p

Kwan JSH, Koo RCH, Ng CWW (2015) Landslide mobility analysis for design of multiple debris-resisting barriers. Can Geotech J 52(9):1345–1359. https://doi.org/10.1139/cgj-2014-0152

Liu H (2019) Impact mechanisms of debris flow against multiple rigid barriers with basal clearance. PhD thesis, The Hong Kong University of Science and Technology, HKSAR, China. https://doi.org/10.14711/thesis-991012752655103412

Liu H, Choi CE, Poudyal S, Jia Z, Ng CWW (2023) A new overflow number for analysing and designing dual rigid barriers with basal clearance. J Geotech Geoenviron (under-review)

McDougall S, Hungr O (2004) A model for the analysis of rapid landslide motion across three-dimensional terrain. Can Geotech J 41(6):1084–1097. https://doi.org/10.1139/t04-052

Ng CWW, Choi CE, Song D, Kwan JSH, Koo RCH, Shiu H, Ho KKS (2015) Physical modeling of baffles influence on landslide debris mobility. Landslides 12(1):1–18. https://doi.org/10.1007/s10346-014-0476-y

Ng CWW, Choi CE, Liu LHD, Wang Y, Song D, Yang N (2017) Influence of particle size on the mechanism of dry granular run-up on a rigid barrier. Géotechnique Letters 7(1):79–89. https://doi.org/10.1680/jgele.16.00159

Ng CWW, Choi CE, Majeed U, Poudyal S, De Silva W (2019) Fundamental framework to design multiple rigid barriers for resisting debris flows. In: Proceedings of the 16th Asian regional conference on soil mechanics and geotechnical engineering. Taipei, Taiwan, pp. 1–11

Ng CWW, Choi CE, Liu H, Poudyal S, Kwan JSH (2020a) Design recommendations for single and dual debris flow barriers with and without basal clearance. In: Sassa K, Mikoš M, Sassa S et al (eds) Understanding and reducing landslide disaster risk. Springer International Publishing, Cham, pp 33–53. https://doi.org/10.1007/978-3-030-60196-6_2

Ng CWW, Wang C, Choi CE, De Silva WARK, Poudyal S (2020b) Effects of barrier deformability on load reduction and energy dissipation of granular flow impact. Comput Geotech 121:103445. https://doi.org/10.1016/j.compgeo.2020.103445

Ng CWW, Liu H, Choi CE, Kwan JSH, Pun WK (2021a) Impact dynamics of boulder-enriched debris flow on a rigid barrier. J Geotech Geoenviron 147(3):04021004. https://doi.org/10.1061/(ASCE)GT.1943-5606.0002485

Ng CWW, Majeed U, Choi CE, De Silva WARK (2021b) New impact equation using barrier Froude number for the design of dual rigid barriers against debris flows. Landslides 18:2309–2321. https://doi.org/10.1007/s10346-021-01631-7

Ng CWW, Choi CE, Liu H, Wang C, Kwan JSH (2021c) Impact mechanisms of debris flow on barriers: modelling, analysis and design. In: SCG-XIII International Symposium on Landslides. ISSMGE, Cartagena

Ng CWW, Yang B, Liu ZQ, Kwan JSH, Chen L (2021d) Spatiotemporal modelling of rainfall-induced landslides using machine learning. Landslides 18:2499–2514. https://doi.org/10.1007/s10346-021-01662-0

Ng CWW, Bhatta A, Choi CE, Poudyal S, Liu H, Cheung RWM, Kwan JSH (2022a) Effects of debris flow rheology on overflow and impact dynamics against dual-rigid barriers. Géotechnique 1–14. https://doi.org/10.1680/jgeot.21.00226

Ng CWW, Liu H, Choi CE, Bhatta A, Zheng M (2022b) Effects of basal clearance on the impact dynamics of dry granular flow against dual rigid barriers. Can Geotech J 59(7):1161–1174. https://doi.org/10.1139/cgj-2020-0682

Ng CWW, Jia Z, Poudyal S, Bhatta A, Liu H (2023a) Two-phase MPM modelling of debris flow impact against dual rigid barriers. Géotechnique 1–14. https://doi.org/10.1680/jgeot.22.00199

Ng CWW, Choi CE, Liu H, Poudyal S, Bhatta A, De Silva WARK, Cheung RWM (2023b) Class A prediction symposium on debris flow impact forces on single and dual barriers. HKIE Transactions (accepted)

NILIM (2016) Manual of technical standards for establishing Sabo master plan for debris flow and driftwood: Technical note of NILIM, no.905. National Institute for Land and Infrastructure Management Sabo Planning Division Sabo Department, Japan, 84 p

Ozturk U, Bozzolan E, Holcombe EA, Shukla R, Pianosi F, Wagener T (2022) How climate change and unplanned urban sprawl bring more landslides. Nature 608(7922):262–265. https://doi.org/10.1038/d41586-022-02141-9

Piton G, Recking A (2016) Design of sediment traps with open check dams. I: hydraulic and deposition processes. J Hydraul Eng 142(2):04015045. https://doi.org/10.1061/(ASCE)HY.1943-7900.0001048

Song D, Ng CWW, Choi CE, Zhou GGD, Kwan JSH, Koo RCH (2017) Influence of debris flow solid fraction on rigid barrier impact. Can Geotech J 54(10):1421–1434. https://doi.org/10.1139/cgj-2016-0502

Song D, Choi CE, Ng CWW, Zhou GGD (2018) Geophysical flows impacting a flexible barrier: effects of solid-fluid interaction. Landslides 15(1):99–110. https://doi.org/10.1007/s10346-017-0856-1

SWCB (2019) Soil and water conservation handbook. Soil and Water Conservation Bureau, Taiwan, pp 523

Takahashi T (2014) Debris flow: mechanics, prediction and countermeasures, 2nd edn. CRC Press. (ISBN 9781138073678). 572 p

VanDine DF (1996) Debris flow control structures for forest engineering. Res.Br., BC Min.for., Victoria, BC, Work. Pap 8, 1996

Volkwein A (2014) Flexible debris flow barriers: design and application (WSL reports 18). Swiss Federal Institute for Forest, Snow and Landscape Research WSL, 29 p

Wendeler C, Volkwein A, Roth A, Denk M, Wartmann S (2007) Field measurements and numerical modelling of flexible debris flow barriers. In: The fourth international conference on debris-flow hazards mitigation: mechanics, prediction and assessment (DFHM-4). Millpress, Chengdu, pp 681–687

Wendeler C, Volkwein A, McArdell BW, Bartelt P (2019) Load model for designing flexible steel barriers for debris flow mitigation. Can Geotech J 56(6):893–910

World Bank (2022) GFDRR annual report 2022: bringing resilience to scale (English). World Bank Group, Washington, DC

Yik M, Pun WK, Kwok FH, Pho J, Ng CWW (2023) Perceptions of landslide risks and warnings in Hong Kong. Landslides 1–14:1211–1224. https://doi.org/10.1007/s10346-022-02021-3

Zanuttigh B, Lamberti A (2006) Experimental analysis of the impact of dry avalanches on structures and implication for debris flows. J Hydraul Res 44(4):522–534. https://doi.org/10.1080/00221686.2006.9521703

Zhou GGD, Ng CWW (2010) Dimensional analysis of natural debris flows. Can Geotech J 47(7):719–729. https://doi.org/10.1139/T09-134